CrossMark

Experimental research on strata movement characteristics of backfill–strip mining using similar material modeling

Xiaojun Zhu [1,2] · Guangli Guo [2] · Hui Liu [1,2] · Tao Chen [2] · Xiaoyu Yang [3]

Abstract

In consideration of the high filling costs and backfill material shortage at present, backfill–strip mining, which combines the advantages of strip mining and backfill mining, has gradually been adopted to control surface subsidence. In this study, similar material modeling is established to simulate strata movement characteristics of backfill–strip mining. The displacement and deformation values of this similar material modeling are precisely acquired through close-range photogrammetry and optical image methods, respectively. On this basis, structural and movement characteristics of the overlying strata are investigated in different stages to reveal the strata subsidence control mechanism of backfill–strip mining. The dynamic deformation characteristics of the overlying strata in mining are also explored. This study provides a scientific technical reference for safe mining engineering design and surface disaster protection for backfill–strip mining.

Keywords Backfill-strip mining · Similar material modeling · Strata movement characteristics · Subsidence control mechanism

Introduction

Surface subsidence—surface elevation falls down due to underground mining—is the most common disaster in mining areas; it results in a series of environmental geological problems (Qian and Xu 2006; Marschalko et al. 2015). According to statistics, surface subsidence has occurred in 20 provinces in China (Xu et al. 2004), especially in Shanxi, Anhui, Heilongjiang, and Shandong provinces. The total damaged land area reached 2 million ha in China. Simultaneously, abundant coal resources under buildings, railways, and water bodies affect the stable production and sustainable development of the coal mines, especially in Eastern China (Cui et al.

2016). For example, approximately 1949 villages are located above the coal resources, which are 60% of all coal resources in Shandong Province.

Many technologies can be applied to control mining subsidence to ensure safety and achieve environmental protection goals. Subsidence control technologies can be divided into two classes (Lokhande et al. 2005; Chen et al. 2016), namely, partial mining technology and backfilling mining technology. The partial mining technology based on coal pillar support controls the displacement of the strata throughout the zone of mining influence, and this technology mainly includes strip mining, room-pillar mining, and roadway mining (Dehghan et al. 2013; Ghasemi et al. 2014). In these partial mining methods, apparent differences exist in the shapes and the loading states of coal pillars. For example, the coal seam of strip mining is generated into regular strips that are mined alternately, and several strip coal pillars are left to support the overlying strata. Among these methods, strip mining is widely applied in China. However, this technology has the disadvantage of low recovery ratio and wastes enormous coal resources. The backfilling mining technology based on filling body support mainly includes gob, caving zone, and separated-bed filling (Zha et al. 2011). In these backfilling mining methods, apparent differences exist in the location of filling body. However, this technology has the disadvantages of high filling costs and backfill material shortage.

✉ Xiaojun Zhu
zhuxiaojunahu@126.com

1 School of Resources and Environmental Engineering, Anhui University, Hefei 230601, People's Republic of China

2 School of Environment Science and Spatial Information, China University of Mining and Technology, Xuzhou 221008, People's Republic of China

3 Department of Engineering Management, Hefei College of Finance and Economics, Hefei 230601, People's Republic of China

(a) First stage of backfill–strip mining

(b) Second stage of backfill–strip mining
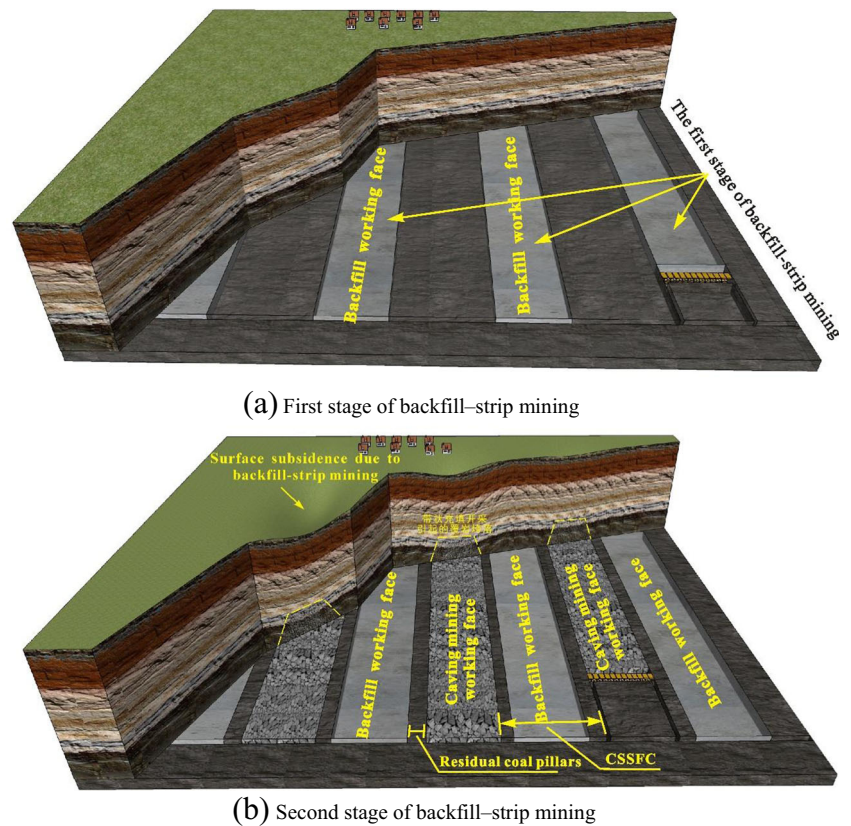
A new concept of backfill–strip mining method is proposed on the basis of the "three-step" mining subsidence control (Guo et al. 2010), which combines the advantages of strip mining and backfilling mining, to address the problems of high backfill cost and backfill material shortage. The research on backfill–strip mining technology has not formed a complete research system, as only a few studies have been done. Guo et al. (2004) first proposed the surface subsidence control of "three-step" mining (stripping, mining-gob grouting, and filling-strip pillar mining) based on the principle of load replacement. Liu (2014) analyzed the feasibility of wide working face in backfill–strip mining based on surface subsidence values. Fang et al. (2013) analyzed the surface subsidence of different mining width and retaining width in backfill–strip mining. Meanwhile, some partial backfilling mining projects whose strata support structures were similar to that of backfill-strip mining have been implemented in Bucun (Sun and Li 2008), Xuchang (Xuan et al. 2013), and Daizhuang coal mines (Xu et al. 2004). The success of these projects provides some evidence that backfill–strip mining is feasible. The abovementioned studies focused on the feasibility of backfill–strip mining. However, the structural characteristics of the overlying strata and strata subsidence control mechanism were not emphasized.
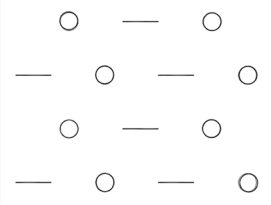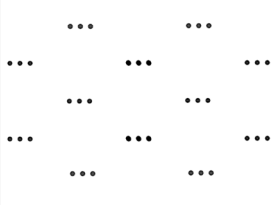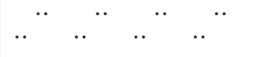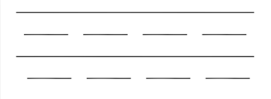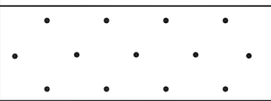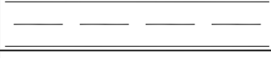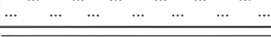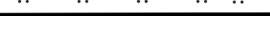
In this paper, the section "Brief overview on backfill–strip mining technology" introduces the specific mining procedures of the backfill–strip mining technology. Backfill–strip mining technology is still in the industrial test stage. So the field measurement data of the surface subsidence have not been acquired. Thus, a similar material model is applied to study the strata movement characteristics in backfill–strip mining. The section "Similar material modeling" describes the laboratory equipment of the similar material modeling and two observation methods of model deformations. The structural and movement characteristics of the overlying strata are investigated in different stages through a similar material simulation method to reveal the strata subsidence control mechanism of backfill–strip mining in the section "Structural characteristics and movement process of the overlying strata in backfill–strip mining". Ultimately, the dynamic displacement and deformation characteristics of the overlying strata in mining are also studied in the section "Dynamic strata movement and deformation characteristics in backfill–strip mining".
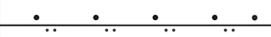
Brief overview on backfill–strip mining technology

Backfill–strip mining is a partial backfilling mining technology that combines the advantages of strip mining and backfilling mining to control strata subsidence. In backfill–strip mining, the coal mining area has a scientific layout of longwall backfilling working faces and longwall caving mining working

Fig. 2 Diagram of simplified geological stratum

STRATA	THICKNESS	GRAPHIC LOG
Top soil	80 m	
Siltstone	80 m	
Medium-grained sandstone	24 m	
Shale	38 m	
Arenaceous shale	50 m	
Shale	26 m	
Sandstone	36 m	
Shale	20 m	
Siltstone	15 m	
Mudstone	18 m	
Sandstone	12 m	
Medium-grained sandstone	12 m	
Coal Seam	2.7 m	
Medium-grained sandstone	15 m	

faces to protect ground targets (e.g., buildings, structures, and farmlands). The specific mining procedures of backfill–strip mining (Fig. 1) are as follows. First, backfilling mining is performed with certain space intervals (Fig. 1a). Second, the coal pillars between backfilling working faces are recycled through the caving mining method when the backfill materials achieve a certain bearing capacity (Fig. 1b). The small residual coal pillars between the gob and backfill materials are not excavated to control roadway deformation and protect the stability of the backfill materials. This mining process eventually forms a combined support structure of filling body and coal pillar to reinforce the overlying strata and achieves the goal of subsidence control. The backfill–strip mining area is composed of backfill mining working faces and caving mining working faces, which are different from backfilling mining and strip mining. Therefore, the characteristics of strata deformation in backfill–strip mining are significantly different from those in strip mining and backfilling mining; thereby, requiring further in-depth study.

Similar material modeling

Site description

Yangzhuang Coal Mine is located in Huaibei City, Anhui Province, China. The topography is flat, and numerous

Table 1 Mechanical parameters of the model and its prototype

Rock type	Prototype parameters			Model parameters		
	Thickness (m)	Compressive strength (MPa)	Tensile strength (MPa)	Thickness (cm)	Compressive strength (MPa)	Tensile strength (MPa)
Top soil	80	3.26	0.40	27	0.0068	0.0008
Siltstone	80	35.87	2.80	27	0.0747	0.0058
Medium-grained sandstone	24	40.36	1.40	8	0.0841	0.0029
Shale	38	18.60	0.98	13	0.0388	0.0020
Arenaceous shale	50	26.47	0.9	17	0.0551	0.0019
Shale	26	18.60	0.98	9	0.0388	0.0020
Sandstone	36	42.50	1.40	12	0.0885	0.0029
Shale	20	18.60	0.98	7	0.0388	0.0020
Siltstone	15	35.87	2.80	5	0.0747	0.0058
Mudstone	18	10.44	0.80	6	0.0218	0.0017
Sandstone	12	42.50	1.40	4	0.0885	0.0029
Medium-grained sandstone	12	30.36	0.84	4	0.0633	0.0018
Coal	2.7	11.50	0.60	1	0.0240	0.0013
Medium-grained sandstone	15	52.50	1.80	5	0.1094	0.0038

residential buildings are located above this mining area. Statistics show that the recoverable coal reserves located under residential buildings are estimated at 20.8 million tonnes; thereby, severely limiting the serving period of the coal mine. Backfilling mining technology was applied in the original design of the coal mine to exploit the coal seam and prevent damage of the ground buildings. However, the filling cost is relatively high. If the buildings above the mining area were to

be relocated, then the relocation costs would be exceedingly high. Therefore, backfill–strip mining is attempted to extract coal resources under the buildings and reduce filling cost.

Due to a lack of actual subsidence measured data, the geological and mining conditions in the coal mine are modeled in the present experiment using the similar material model. The simulated structure of the overlying strata was appropriately simplified on the basis of the actual borehole columnar section
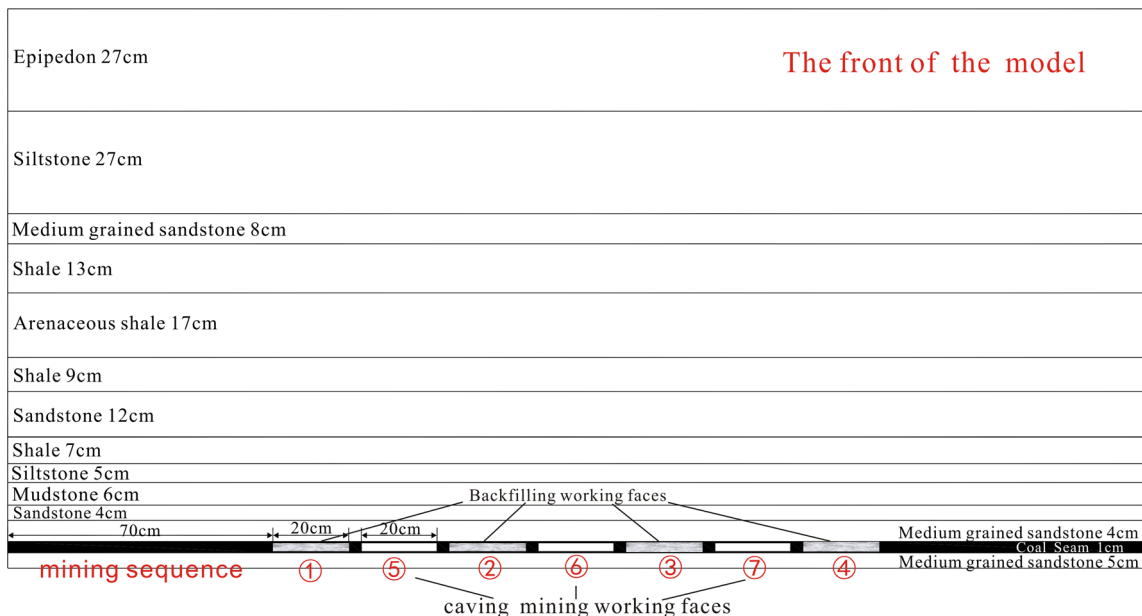

Fig. 3 Design chart of the similar material model

Table 2 Material proportions in the similar material model

Rock type	Sand (%)	Mica powder (%)	Plaster (%)	Calcium carbonate (%)
Top soil	94	4	0.6	1.4
Siltstone	93	4	2.1	0.9
Medium-grained sandstone	92	4	2.8	1.2
Shale	92	5	1.2	1.8
Arenaceous shale	93	4	1.5	1.5
Shale	92	5	1.2	1.8
Sandstone	92	4	2.8	1.2
Shale	92	5	1.2	1.8
Siltstone	92	4	2.4	2.4
Mudstone	91	6	1.8	2.1
Sandstone	92	4	2.8	1.2
Medium-grained sandstone	93	4	1.5	1.5
Coal	93	4	2.1	0.9
Medium-grained sandstone	89	3	5.6	2.4

of Yangzhuang Mine and test conditions. The graphic log of the simplified strata structure is illustrated in Fig. 2. The immediate roof and floor are made of medium-grained sandstone, and the No. 6 coal seam is conducted to simulate excavation, with average thickness and depth of 2.7 and 400 m, respectively.

Laboratory equipment and similarity parameters

Similar material modeling is a scale physical model constructed using simulation materials based on scale model theory (Peng 2013). The strata movement data of the model are measured and converted to actual values for comparative and critical analysis (Gao et al. 2008). This simulation method is easier and quicker than field measurement and can make up for limitations of field measurement with its advantages of short experimental period, low cost, and visual results. Thus, many scholars have used similar material modeling to successfully simulate the structures, failure modes, and movement processes of the overlying strata, much like those observed in underground coal mines. Mitchell et al. (1982) analyzed the stability problem of cemented tailing backfill using similar material modeling. Gao et al. (2008) studied the time series system of artificially-induced caving of safety roof during continuous mining in ore body No. 92 of Tongkeng Tin Mine with similar material modeling. Wu et al. (2015) simulated the dynamic movement of the overlying strata during coal mining using similar material modeling. He

and Yang (1991), Gu (1995), and Li (1988) studied the mixed proportion of similar materials using the mechanical experiment based on the actual physical and mechanical properties of rocks. Therefore, similar material modeling is one of the most effective methods for studying ground and strata destruction induced by underground coal exploitation, and it is feasibly established in this study to simulate strata movement of the backfill–strip mining.

Based on the simulation stratum diagram and experimental conditions, a similar material modeling experiment was implemented on iron shelves with a dimension of 300 mm × 300 mm × 1400 mm (length × width × height). To reflect the important physical properties of the prototype (e.g., mechanical and kinetic characters), the similar material model and actual geological environment must follow three similarity theorems (Ghabraie et al. 2015), namely, geometric similarity, kinematic similarity, and mechanical similarity, to ensure that the physical model is proportional to the prototype system.

Geometric similarity ratio c_l, which is described in Eq. (1), is the ratio between the sizes of the physical model and the prototype.

$$c_l = L_m/L_p, \qquad (1)$$

where L_m and L_p are the lengths of the model and the prototype, correspondingly. The geometric similarity ratio of model α_l was set to 1:300 according to the simulation mining scope and sizes of the panel shelves.

Table 3 Mechanical parameters of the cemented backfill material

Concentration (%)	Gangue (%)	Coal ash (%)	Lime (%)	Cement (%)	UCS (MPa)			
					1 d	3 d	7 d	28 d
75	45.5	40	12	2.5	0.25	0.82	1.69	2.92

Fig. 4 Similar material specimen

Fig. 5 UCS contrast curves of the actual cemented and similar materials

Kinematic similarity, which is described in Eq. (2), maintains the movement time of each corresponding point between the physical model and the prototype system in proportion.

$$c_t = t/T, \tag{2}$$

where c_t is the time similarity ratio, and t and T are the movement times of the model and prototype, respectively. The time similarity ratio c_t is related to geometric similarity ratio c_l and can be expressed by $c_t = \sqrt{c_l}$. In this test, the time similarity ratio c_t is 1:17.3.

Mechanical similarity ensures similarity in the mechanical properties between the prototype and the model systems. Mechanical similarity ratio c_δ can be calculated using Eq. (3).

$$c_\delta = c_\rho \cdot c_l, \tag{3}$$

where c_ρ is the density ratio of the similar material to the rock. The similar material is composed primarily of sand, and its density is 1500 kg/m³. Thus, the density similarity ratio c_ρ =1:1.6 and the mechanical similarity ratio c_δ is 1:480.
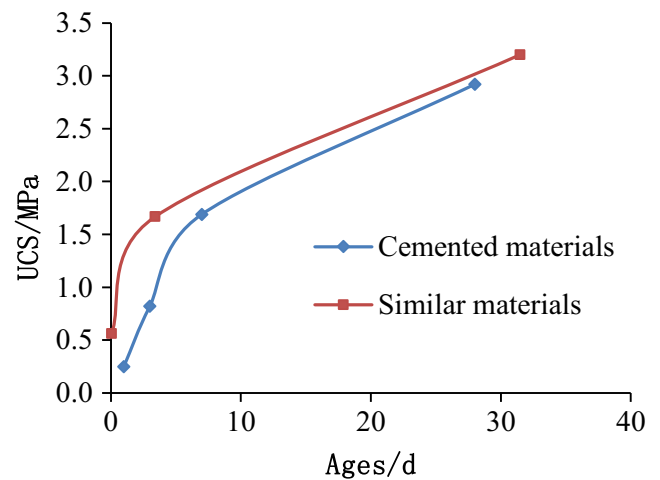
Mechanical parameters of the model were determined (Table 1) based on strength parameters of the various strata and similarity ratio.

The similar material model simulates 2D displacement and deformation of strata in backfill–strip mining along the direction of the dip section (under the assumption that the strike length of the working faces reached the critical size). The actual widths of the backfilling working faces and caving mining working faces are 60 m, and the actual width of the barrier pillar is 10 m. The simulation mining process of the model can be divided into two stages. In stage I, the similar material model adopts backfilling mining from left to right seen from the front of the model, and each backfilling working face is filled immediately after being mined. In stage II, residual pillars are mined through the caving mining method after completing stage I, and 10 m width barrier pillars are reserved between the caving mining and backfilling working faces. The design chart of the similar material model is depicted in Fig. 3. Four backfilling working faces and three caving mining working faces were simulated using the similar material model.

The similar materials of the strata are compounds and are mainly composed of dry sand, mica powder, plaster, light calcium carbonate, and water. Rock formation plasticity was controlled by adjusting the mix ratio of mica powder. Cementing materials are mainly composed of plaster and calcium carbonate. Different strengths of the similar materials can be achieved by regulating the ratio of the plaster to calcium carbonate on the same cement–sand ratio conditions. Borax was added to prevent rapid solidification of the cementing materials to ensure sufficient time to prepare the model; sawdust was added to soften the topsoil.

The weight of different materials can be calculated (Table 2) according to the mechanical parameters of the model and empirical formula of the tensile and compressive strengths of the different proportions of similar materials in the literature (He and Yang 1991).
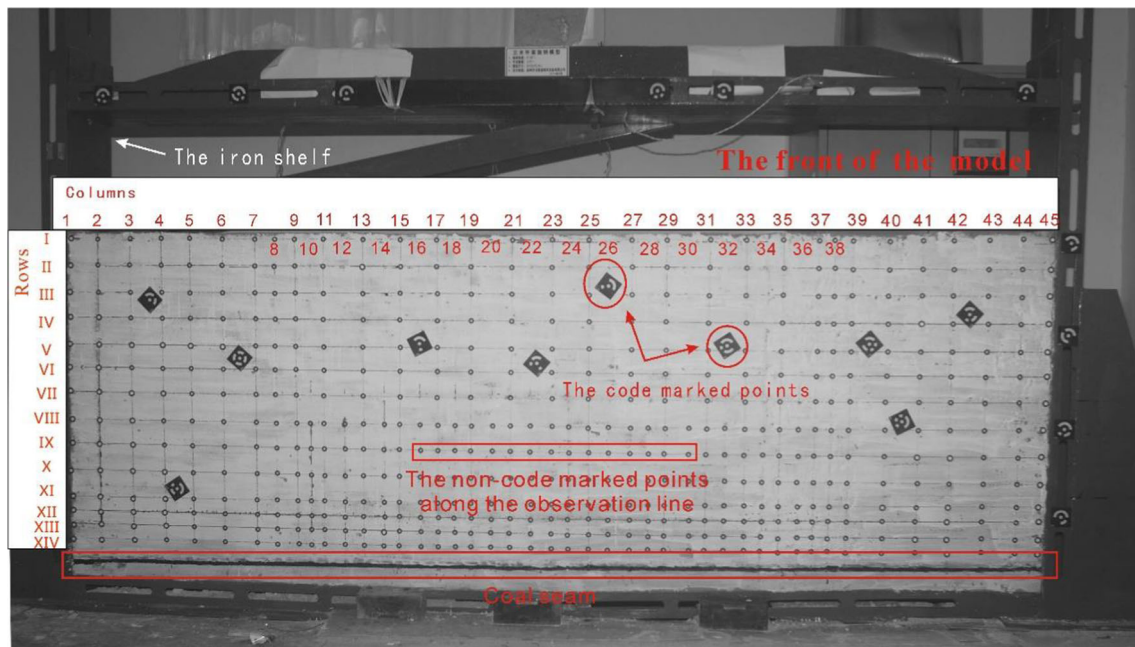
Fig. 6 Layout of the model monitoring points for close-range photogrammetry system

Mixture ratio of backfill similar material

Similar material modeling of backfill–strip mining requires simulation of not only the strata movement but also the compression deformation process of the backfill similar material. Thus, the final mechanical strength of the backfill similar material should be taken into account, and the change process of the mechanical strength with time also should be considered.

The backfill materials can be divided into solid backfill materials and cemented backfill materials according to the characteristics of the backfill materials. Solid backfill similar materials mainly consider the compressive deformation with the stress change. Zha (2011) used foam and sponge as the similar materials of solid backfill materials and simulated the different stress–strain relationships of solid backfill materials through different thickness ratios of the foam and sponge. However, the cemented backfill similar materials mainly consider the change process of the mechanical strength. Few studies on the cemented backfill similar materials are available. Thus, the mixture ratio of the cemented backfill similar materials to similar materials was studied to accurately simulate the change process of the mechanical strength of the backfill similar materials.

The cemented backfill material selected in this study refered to the proportion of the cemented backfill material of cemented backfilling mining in Gonggeyinzi Coal Mine, Inner Mongolia Autonomous Region, China. The proportion and the mechanical properties of the cemented backfill material are shown in Table 3.

The mechanical strength of the backfill similar materials with time is changed. Thus, the kinematic and mechanical

similarity characteristics of the backfill similar materials should be considered in studying the optimum ratio of similar materials. The uniaxial compressive strength (UCS) of the cemented backfill material is assumed as σ at the time of curing time t, and then the uniaxial compressive strength of the cemented backfill similar material is σ/C_δ at the time of curing time $t/\sqrt{C_l}$ according to the time and mechanical similarity ratios.

Although various materials can be used as the raw materials of the similar material model, the following requirements should be satisfied when selecting the raw materials. The raw materials have stable mechanical behavior, and their mechanical properties are similar to the actual rock. Moreover, the cost is low, and their manufacture is convenient. So, gypsum, additive (mainly composed of sulfates), and water are used as the raw materials for the cemented backfill similar materials given these factors.

The similar materials were made into the standard cylinder specimens with the diameter and height of 50 and 100 mm, correspondingly, (Fig. 4) to determine the mechanical strength of similar materials under different proportions of gypsum, water, and additives. Then, these specimens were compacted using a CSS-55500 compression testing machine to obtain the uniaxial compressive strength of the cemented backfill similar materials. The UCS of the cemented backfill similar materials will be converted to the actual UCS according to the 1:480 mechanical and 1:17.3 time similarity ratios when the experiment is complete.

Numerous mechanical experiments of the cemented backfill similar materials in different proportions have shown that the mechanical characteristics of the cemented backfill similar
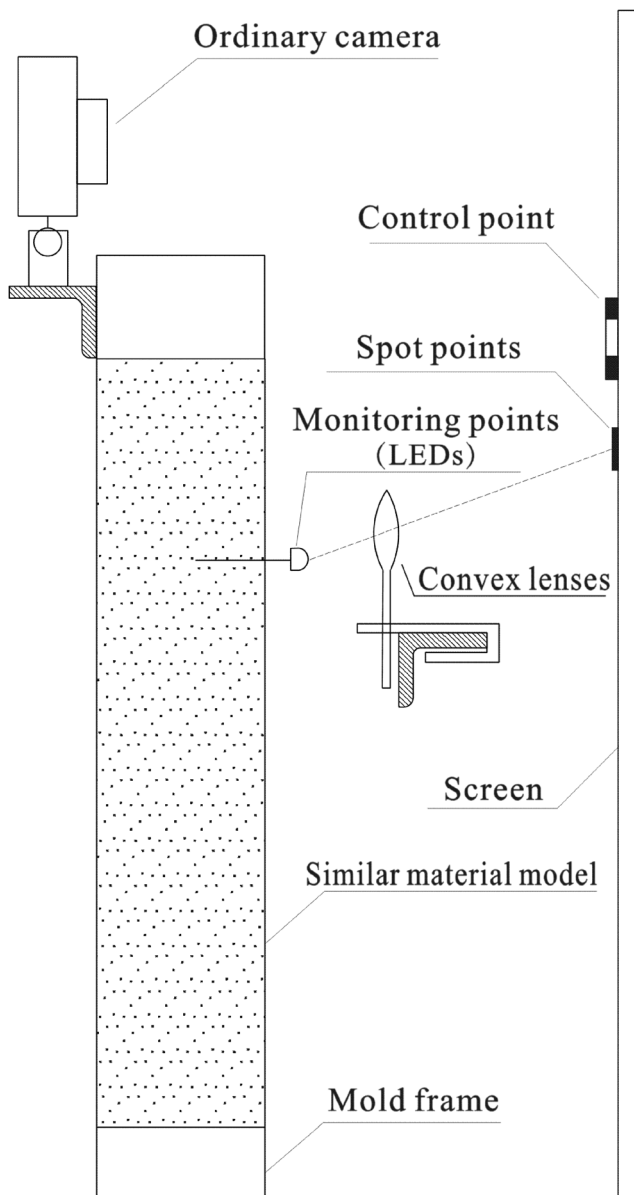
Fig. 7 Schematic of the optical imaging method

materials are the most similar to the actual cemented materials when the ratio of gypsum, additive, and water is 100:5:70. The UCS contrast curves of the different ages of the actual cemented and similar materials are demonstrated in Fig. 5. So, this material proportion can be the proportion of the backfill similar material of the backfill–strip mining.

Observation methods

Two methods, namely, the digital close-range photogrammetry system (Zhang et al. 2010) and optical imaging method (Zhu et al. 2015), were adopted to monitor the strata and surface deformations of the similar material model of the backfill–strip mining.

The digital close-range photogrammetry system is developed based on close-range photogrammetry theory. The monitoring points in this system can be divided into two classes, namely, code and non-code marked points. The code marked points were attached with a certain density distribution on the surface of the model for image mosaics. The non-code marked points were attached on the model to monitor the displacement of the targeted points. The monitoring accuracy of this system is 0.03–0.1 mm. Therefore, the actual monitoring accuracy is 9–30 mm, which could be calculated according to the 1:300 geometric similarity ratio. This accuracy satisfies the measurement precision requirement of the final subsidence of the strata and surface.

According to the stratigraphic structure, survey lines were laid and numbered as I–XIV from top to bottom in the vertical direction and as 1–45 from left to right in the horizontal direction. The interval of the lines is approximately 10 cm. However, the survey lines were laid densely above the coal seam for acquiring additional data. The detailed layout is displayed in Fig. 6. The survey points of the model were observed once every 18 h to acquire comprehensive and systematic strata displacement and deformation data; 14 sets of strata movement data were obtained. The collapse and fracture of the overlying strata were recorded by capturing photographs and sketching during the model excavation process.

The optical imaging method was used to obtain the dynamic displacement of the model with convex lens projection, photogrammetry, and image recognition technology. In this method, light-emitting diodes (LEDs) were used as the monitoring points; the spots of LEDs were projected onto the back screen of the model, and the micro displacements of the LEDs were amplified by the convex lenses. The images of the spots at different times were captured automatically by a camera, and the center coordinates of control and spot points in the images can be extracted through the image recognition method. The plane coordinates of the spot points in the object space can be calculated by 2D direct linear transform, and the displacement of the LEDs on the model can be calculated by lens magnification. The displacement accuracy of the monitoring point of the optical image method is higher than 0.01 mm. The schematic of the optical imaging method is presented in Fig. 7.

The two rows of the monitoring points of the optical imaging method were laid on the back of the similar material model (Figs. 8 and 9) to monitor the dynamic deformation of the strata. The spot points were photographed every 15 min, which was equal to the 0.18-day actual monitoring interval based on time similarity ratio. The model was continuously monitored for approximately 260 h from January 29 to February 9, 2015, and more than 1000 images were obtained to study the strata movement characteristics in the backfill–strip mining.
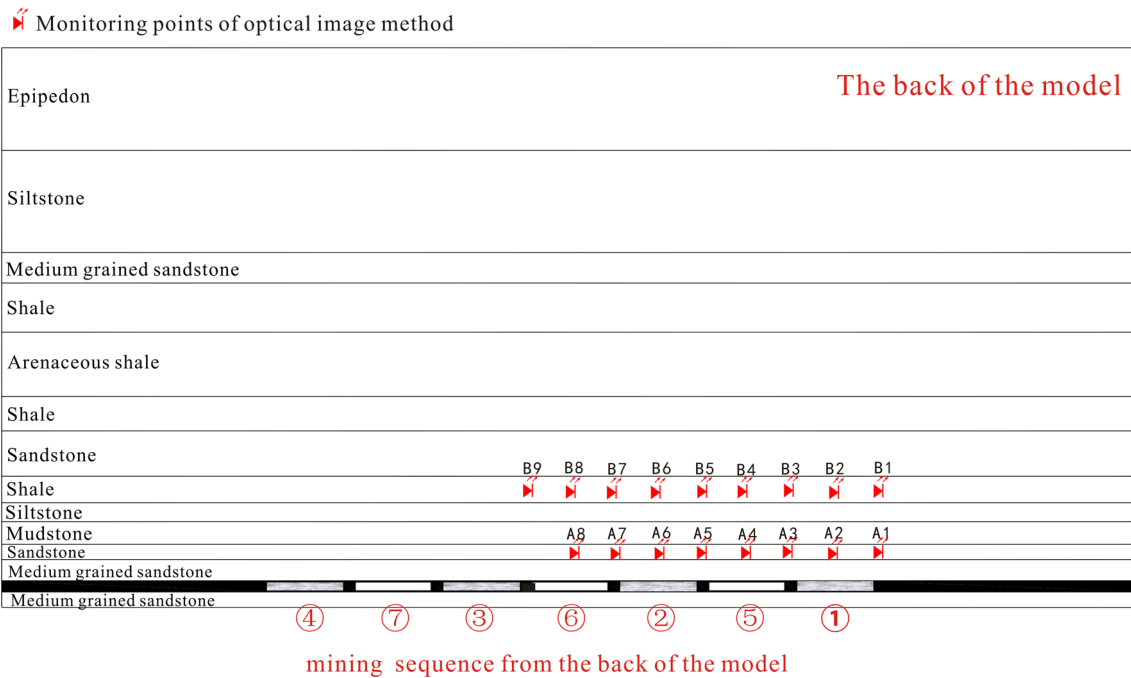
Fig. 8 Layout of the monitoring points in the optical image method

Structural characteristics and movement process of the overlying strata in backfill–strip mining

Structural characteristics and movement process of the overlying strata in stage I of the backfill–strip mining

The overlying strata gradually curved downward to the goaf under the action of the overlying load after extracting coal resources. The roof gradually came into contact with the backfill materials and was supported by the backfill materials because the backfill materials immediately filled into the goaf. The backfill materials were not compressed, and the overlying strata did not subside when the internal stress of the rock mass reached equilibrium. Figure 10 shows the overlying strata structure is mainly in the form of bending deformation in stage I of the backfill–strip mining. No evident caving zone developed in the overlying strata, and only small minor fractures formed in the roof. The height of the fracture zone was approximately 5–12 m. The backfilling mining working faces in stage I of the backfill–strip mining were arranged at certain space intervals, and the coal pillars were reserved with certain widths between the two adjacent working faces. After one backfilling working face was completely mined, the previous overlying strata and rock pressure were not appreciably disturbed by the next backfilling working face because of the barrier of the wide coal pillar. The overlying strata were slightly damaged, and the damage height of the overlying strata was lower. Meanwhile, the backfill materials were laterally restricted by the coal pillars that acted as the retaining walls;

thereby, further increasing the strength of the backfill materials and reducing the strata subsidence.

The final subsidence curves of the strata are depicted in Fig. 11, and the subsidence curves of the two typical
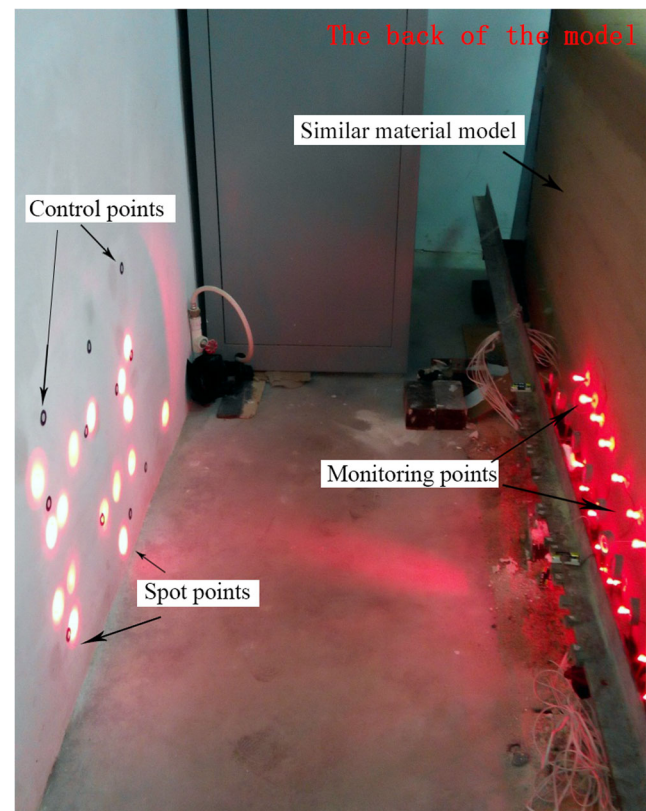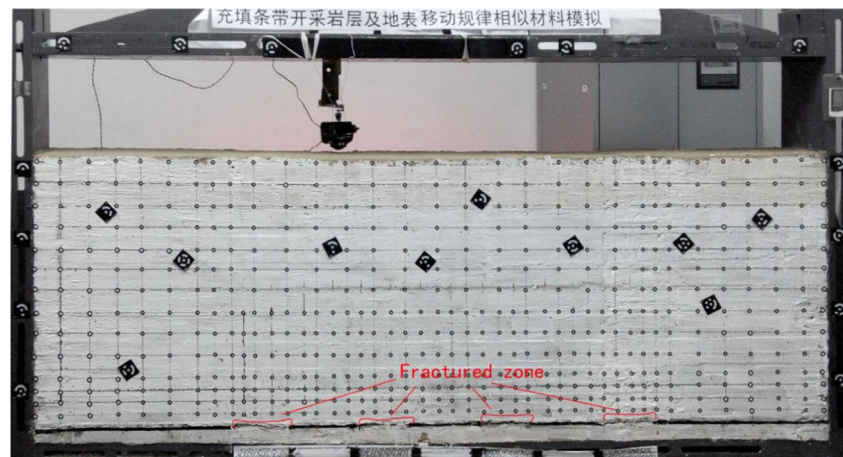

Fig. 9 Actual monitoring chart of the optical imaging method on the back of the model

Fig. 10 Structural characteristics of the overlying strata in stage I of backfill–strip mining


monitoring lines (surface and Line XIV) after the different backfilling working faces are illustrated in Figs. 12 and 13. The formation process of surface subsidence indicates that the subsidence gradually spreads in the vertical direction from the goaf to the surface. Finally, a subsidence basin on the surface is formed, and the extent is larger than the goaf. The subsidence superposition degree of the strata at different elevations is different in the transfer process of subsidence space given the special spatial layout of the backfill–strip mining. Thus, the wavy subsidence shape and smooth subsidence curves existed simultaneously in the overlying strata. In Figs. 11 and 13, the subsidence caused by the four backfilling working faces is less superimposed on the subsidence curves of the strata location on survey lines XIV and XI because these strata were close to the coal seams, and the backfilling working faces were divided by wide coal pillars. Then, a concave subsidence curve was formed under the mining influence of each backfilling working face, and the subsidence curves of these strata were ultimately displayed as wavy subsidence shapes with peaks over each backfilling working face and valleys over the coal pillars. In Figs. 11 and 12, by contrast, the subsidence curves of the strata that were distant from the coal

seams present smooth scoop shapes under the superimposing influence of the backfilling working faces.

The overlying strata in stage I of the backfill–strip mining can be divided into two zones, namely, synchronous bending zone and wavy bending zone, according to the subsidence form of the strata (Fig. 14). When several backfilling faces divided by wide coal pillars were mined, the subsidence curves of the strata near the coal seams were wavy, and the zone of the rock strata was defined as "wavy bending zone" in this paper. However, the subsidence curves of the strata, which are far from the coal seams, showed subsidence basins, and the zone of the rock strata was defined as "synchronous bending zone".

Figure 15 shows that the subsidence values of the monitoring points above the coal pillar in the wavy bending zone increased with the increase in distance from the coal seam, whereas those in the synchronous bending zone decreased with the increase in distance from the coal seam. The monitoring points above the coal pillars and the backfilling working face subsided synchronously when the distance from the coal seam reached 150 m. Thus, the synchronous bending zone is the area of the overlying rock strata above the 300 m

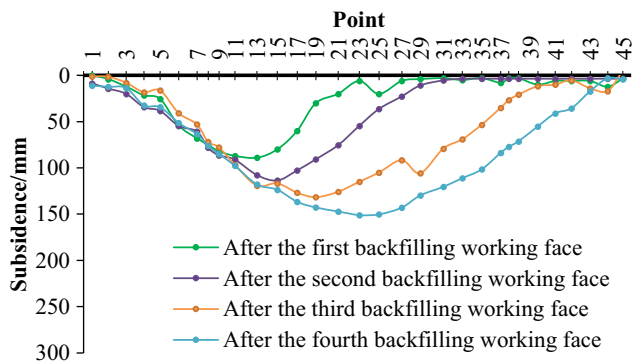**Fig. 11** Strata subsidence curves after stage I of the backfill–strip mining
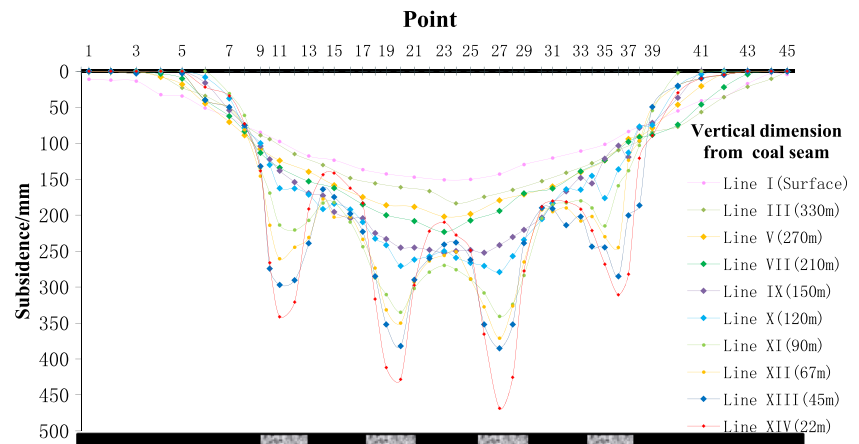
Fig. 12 Surface subsidence curves after the different backfilling faces
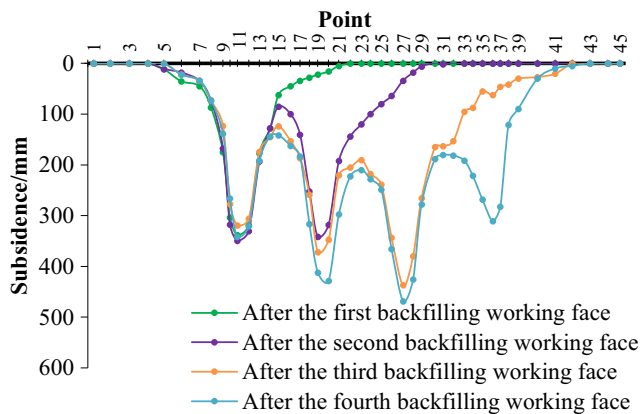

Fig. 13 Subsidence curves of line XIV after the different backfilling working faces

distance from the coal seam in stage I of the backfill–strip mining.

The decrease rate of the subsidence values of the monitoring points was considerably greater in the wavy bending zone than in the synchronous bending zone. This phenomenon was attributed to the rock strata in the wavy bending zone that were affected by the non-uniform vertical stress, which consequently resulted in the bend of the overlying strata. The large bending deformation resulted in the interlayer detachment and separation of the strata. Some voids were created between the strata. Therefore, the subsidence reduction of the strata was large. However, the strata in the synchronous bending zone presented a gentle subsidence curve and only indicated
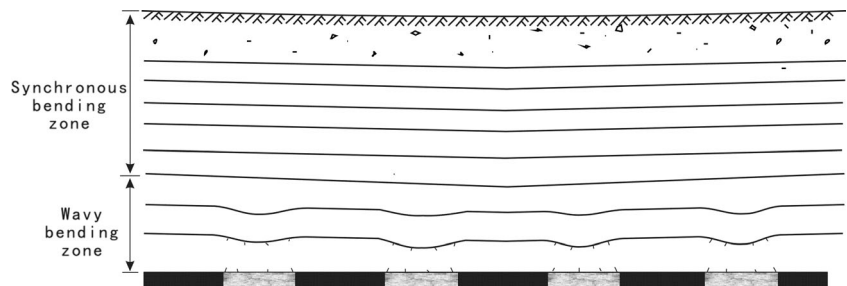
minimal bending deformation and few small interlayer detachments. Thus, the subsidence reduction of the strata in the synchronous bending zone was relatively minimal.

Structural characteristics and movement process of the overlying strata in stage II of the backfill–strip mining

Figure 16 indicates that the roof of every caving mining working face after stage II of the backfill–strip mining lost the support of coal pillars and collapsed when the goaf was enlarged to a certain size, and the load of the overlying strata exceeded the roof strength. Three separate arched caving zones, which were similar to the arches of the bridge, were formed in the inclination major section. The shape of the rock strata above the backfilling working faces was inverted trapezoid and was similar to the bridge piers that supported the load of the overlying strata. The caving zone continuously developed upward until the siltstone from the coal seam was approximately 16 m high. The overlying strata were supported by the rock beam. The size of working face was small, and the overlying strata were supported by coal pillars and filling body on both sides. Thus, the broken rock was insufficient for filling the goaf, and did not touch the overlying strata that were not caved. A large space was left behind in the caving zone and cannot be filled by the broken rock. The height of the caving zone was approximately two to three times the mining thickness and less than the height of the caving zone when the working faces reached the critical size. The caving angle was approximately 40–51°. The height of the fracture zone was approximately ten times the mining thickness.

Figure 17 shows the subsidence curves of the different survey lines after stage II of the backfill–strip mining. Figures 18 and 19 demonstrate the subsidence curves of the surface and line XIV after the different caving working faces, respectively. The subsidence of the overlying strata sharply increased after stage II of the backfill–strip mining. The rock strata near the coal seam produced three high subsidence peaks at the same location of the valley of the wavy subsidence curves in stage I. The peak values of survey line XIV over the mining faces were 1816, 2100, and 1832 mm, and the location of the maximum peak value was over the second mining working face. The maximum peak value was

Fig. 14 Classified schematic of the overlying strata in stage I of the backfill–strip mining

Fig. 15 Subsidence values of the rock strata in different distances above the coal pillar and backfilling working faces
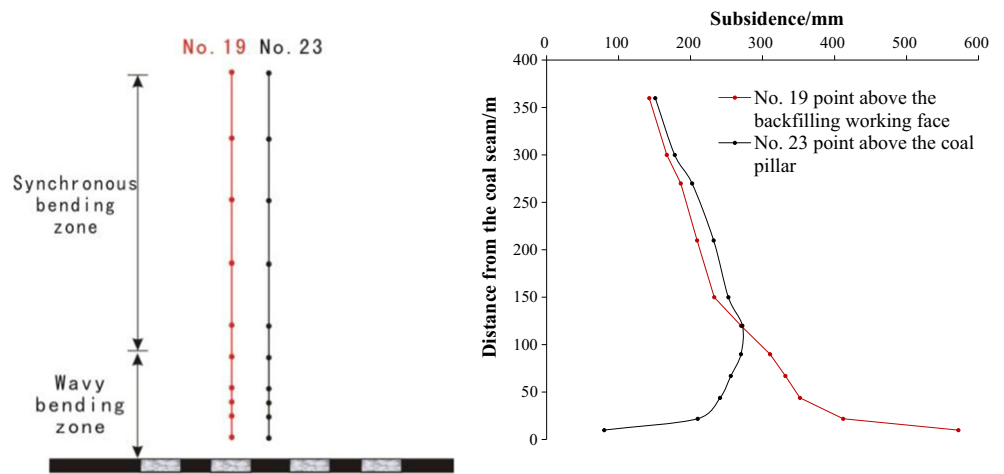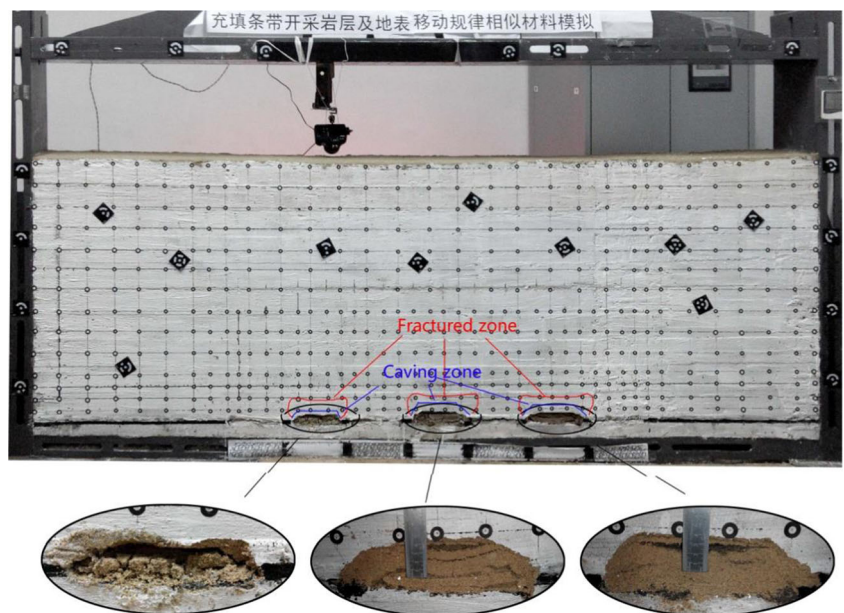

Fig. 16 Structural characteristics of the overlying strata in stage II of the backfill–strip mining

considerably greater than that in stage I. With the increase in distance between the survey line and the coal seam, the mining-induced subsidence decreased and the peak-to-valley subsidence difference value of the wavy subsidence curves of

Fig. 17 Strata subsidence curves after stage II of the backfill–strip mining
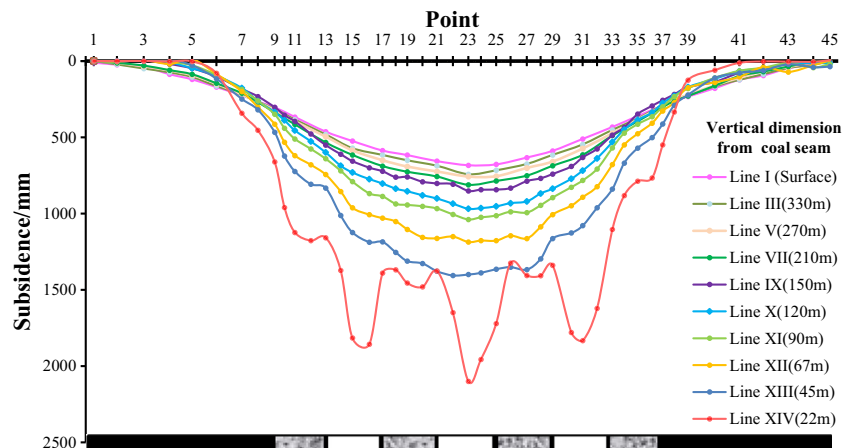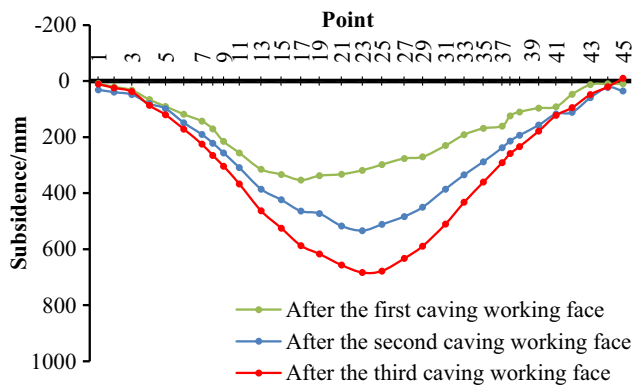
Fig. 18 Surface subsidence curves after the different caving working faces
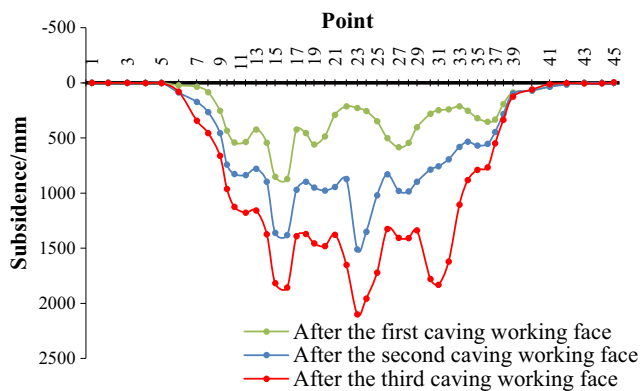

Fig. 19 Subsidence curves of line XIV after the different caving working faces

the survey line gradually decreased. The subsidence curves gradually flattened and formed a single subsidence basin until survey line XIII (45 m from the coal seam). The maximum subsidence of the surface subsidence curves in stage II increased sharply from 209 mm in stage I to 745 mm.

The overlying strata in stage II of the backfill–strip mining can be divided into three zones according to the subsidence form of the strata. These three zones are the arched caving zone, wavy bending zone, and synchronous bending zone (Fig. 20). Each caving mining working face in stage II of the backfill–strip mining caused large damage to the overlying strata. The damage caused by backfill mining to the overlying

strata in stage I of the backfill–strip mining was small. Thus, the strata of the synchronous bending zone and the wavy subsidence zone above the goafs depended on several inverted trapezoidal "piers," and the two sides of the "piers" are surrounded by the caving rock mass. This zone is called "arched caving zone."

In Fig. 21, the height of the arched caving zone in stage II of the backfill–strip mining was 16 m and the height of the wavy bending zone was 16–45 m. The height and extent of the wavy bending zone sharply decreased compared with those in stage I. The subsidence of each survey point above the barrier coal pillars and backfilling working faces in the wavy bending zone increased with elevation, whereas that in the synchronous bending zone decreased. When the height from the coal seam was 45 m, the subsidence of each survey point above the coal pillars and that above the backfilling working faces decreased synchronously at the same subsidence decay rate.

Strata subsidence control mechanism in backfill–strip mining

The strata movement deformation characteristics of the backfill–strip mining in Figs. 20 and 21 show that two key strata played a role in controlling partial strata deformation, which existed among three subsidence zones. The two key strata were defined as the "main structure stratum" and the "synchronous structure stratum" (Fig. 20) for a better description of strata subsidence control mechanism. The rock stratum that was not caved and rests on the "piers" of the arched caving zone is the "main structure stratum." It existed between the arched caving and wavy bending zones. The rock stratum that hindered the upward spread of the wavy subsidence of the overlying strata is the "synchronous structure stratum," which exists between the wavy and synchronous bending zones.

The maximum surface subsidence is much smaller in the backfill–strip mining than in the traditional caving mining with the same mining height. If the coal seam is mined by the caving mining, then the maximum surface of the predicted subsidence is approximately 2160 mm in the geological and mining conditions of Yangzhuang Coal Mine, which is predicted by the probability integral method. The prediction parameters were selected by referring to the regulation (State

Fig. 20 Classified schematic of the overlying strata in stage II of the backfill–strip mining
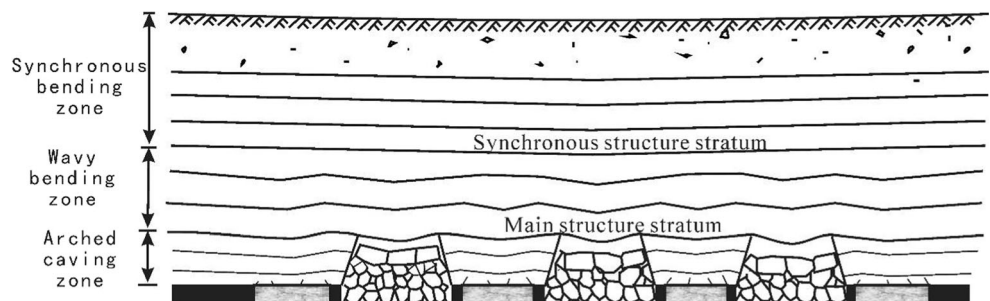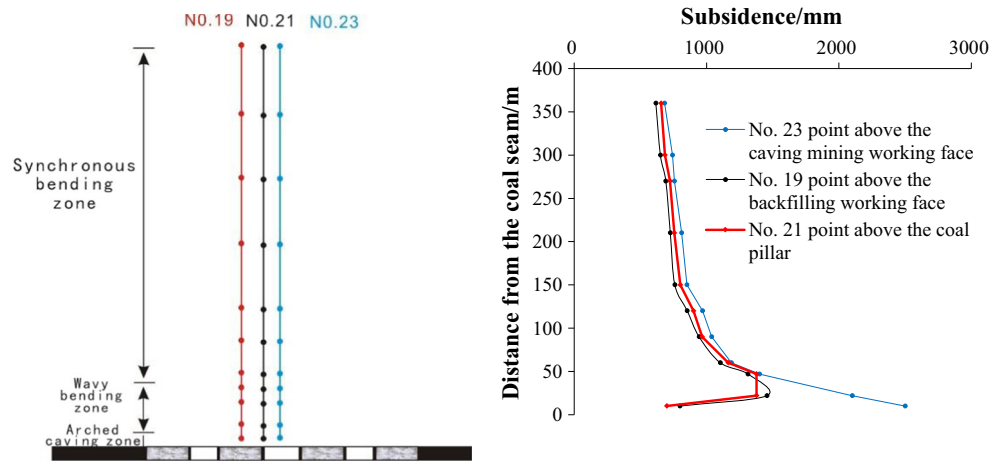
Bureau of Coal Industry 2000). However, the maximum surface subsidence mined by the backfill–strip mining was only 683 mm. Thus, the strata movement deformation characteristics and subsidence control mechanism of the backfill–strip mining are different from those of other mining methods because the combined forms of the overlying strata, filling body, and coal pillars are distinctive. The main structure stratum and synchronous structure stratum formed the two-layer control structure in the strata and controlled the subsidence of the overlying strata synergistically. First, the main structure stratum prevented the strata from caving above itself and significantly decreased the subsidence space spread upward. The synchronous structure stratum hindered the upward spread of the wavy subsidence and smoothened the overlying strata.

The overlying strata above the caving mining working faces broke into blocks without the support of the coal pillars

after excavating the coal seam. However, the overlying strata above the backfilling working faces did not collapse because of the support of the filling body and residual coal pillars, and formed the structure of the bridge piers in the inclination major section to support the main structure stratum. Due to this particular structure, the main structure stratum avoided losing bearing capacity and breaking. The subsidence space of the goaf is effectively blocked by the main structure stratum. Therefore, the main structure stratum could control the subsidence of the strata effectively.

The synchronous structure stratum is generally composed of one or more layers of hard rock. Its elastic modulus is large, strength is high, and bending deformation is small. These factors resulted in desynchronization of the deformation of the synchronous structure stratum with that of the underlying strata. Given these non-synchronous characteristics, the
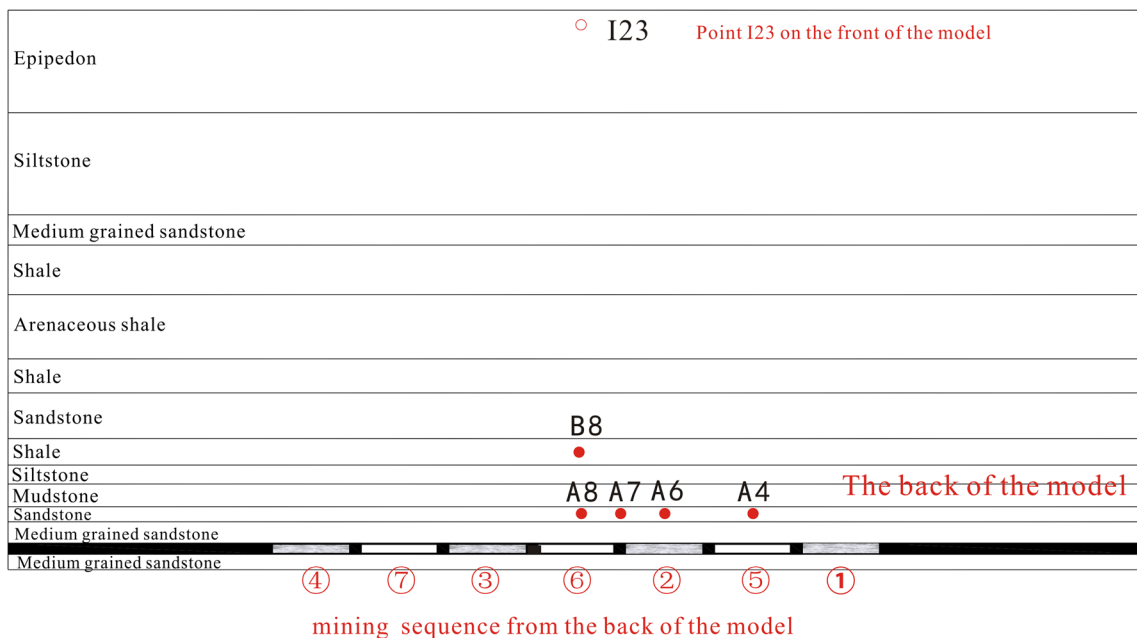

Fig. 22 Layout of the selected points for analyzing dynamic strata movement characteristics
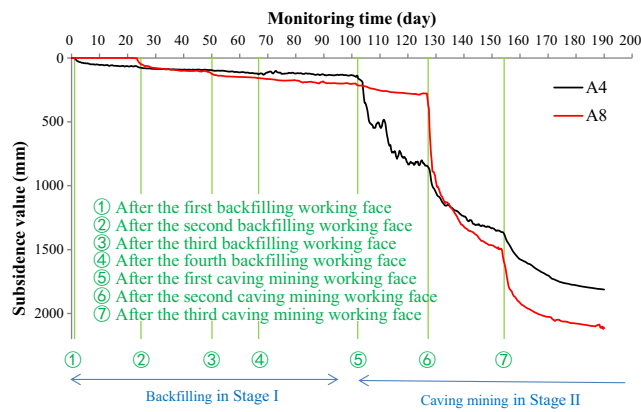
Fig. 23 Dynamic subsidence curves of points A4 and A8 at different positions on the same horizontal stratum

synchronous structure stratum weakened or blocked the transfer of the gap at the interface of the wavy and synchronous bending zones. Therefore, the synchronous structure stratum could reduce the subsidence of the strata and protect the surface buildings and facilities effectively.

Dynamic strata movement and deformation characteristics in backfill–strip mining

Numerous dynamic strata movement values of the points at the back of the model were obtained through the optical imaging method for studying the dynamic strata movement and deformation characteristics in backfill–strip mining. The monitoring days and subsidence values were converted to corresponding prototype data by the similarity ratio for comparison with actual field conditions, as illustrated in Figs. 23, 24, and 25. The subsidence curves of the representative five survey points (Fig. 22) over time were selected to study the dynamic strata movement characteristics. Among the five survey points, points A4, A6, A7, and A8 were on the same horizontal stratum. Point A6 was located over the second backfilling working face. Points A4 and A8 were located over the first
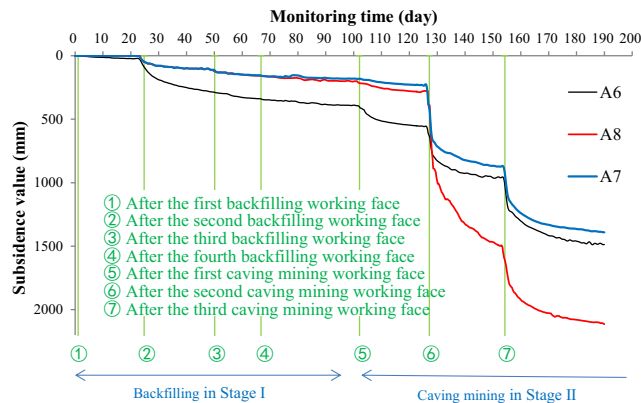

Fig. 24 Dynamic subsidence curves of points A6, A7, and A8 in different positions on the same horizontal stratum
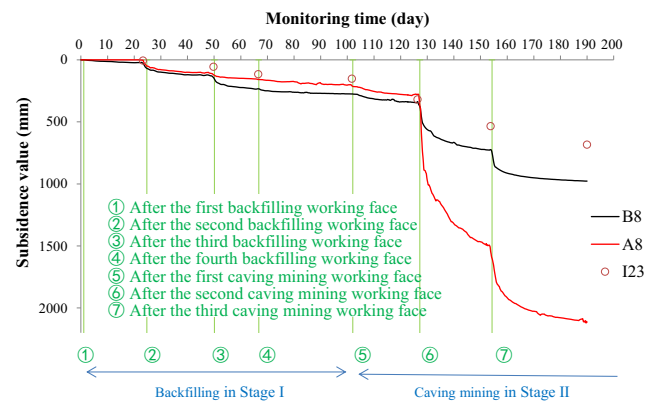

Fig. 25 Dynamic subsidence curves of points A8 and B8 in different positions on the same vertical line

and second caving mining working faces, respectively. Point A7 was located over the residual coal pillar between the second backfilling and the second caving mining working faces. The seven times subsidence values of point I23 (Fig. 22) on the surface obtained by the digital close-range photogrammetry system after the mining of every working face were presented in Fig. 25 to compare the dynamic movement characteristics of the points on the surface and strata. Point I23 was located at the center of the surface on the front of the model. Three survey points (A8, B8, and I23) were selected from the same vertical section.

The common dynamic subsidence characteristics of such points can be obtained from Figs. 23, 24, and 25. All the points during the excavation process of each working face of the backfill–strip mining experienced initial subsidence phase, active subsidence phase, and delayed subsidence phase. The dynamic subsidence curve of each point had seven "ladder-shaped" curves, which corresponded to the extraction process of seven working faces. However, the duration and extent of the "ladder-shaped" subsidence of the different excavation processes were slightly different because of the different spatial relationships between the points and working faces.

In stage I of the backfill–strip mining, most subsidence curves of the survey points were flattened, except for the survey points close to the backfilling working face. The dynamic subsidence process of the survey points distant from the backfilling working face did not indicate an active subsidence phase and clear "ladder-shaped" subsidence curves.

In stage II of the backfill–strip mining, the overlying strata broke violently, and the subsidence values of survey points A4 and A8 were larger than those in stage I. Note that points A4 and A8 were located over the first and second caving mining working faces, respectively. The overlying strata of the second caving mining working face were influenced by the adjacent working faces in the mining process. Therefore, the subsidence value was more violent in survey point A8 during the excavation process of the second caving mining working face than in point A4 on the first caving mining working face, with

an increase in subsidence by 79%. Meanwhile, the subsidence value was more violent in survey point A8 in the same vertical section of the second caving mining working face than in survey points B8 and I23, with an increase in subsidence by 884 and 1431 mm, respectively. Therefore, each point experienced active subsidence phase at each caving mining working face. However, the activity level was related to the breakage extent of the overlying strata and position of the survey point relative to the working face. The breakage in the overlying strata was only above the mining face or the goaf was violent, with a large amount of active dynamic strata subsidence.

Conclusions

A similar material modeling was applied to study the structural, failure, and dynamic displacement characteristics of the overlying strata in the mining process of backfill–strip mining. The following conclusions were obtained.

(1) The structural evolution process of the overlying strata in the backfill–strip mining can be divided into two stages. The overlying strata had favorable integrity in stage I and only exhibited minor fractures on the roof, where the height of the fracture zone was approximately two to four times the mining thickness. The overlying strata above the caving mining working face collapsed consecutively in stage II; thereby, forming several separate arched caving areas. The deformation of each stratum in stage II was remarkably larger than the results in stage I. The section of every caving zone was trapezoid-shaped with a height two to three times the mining thickness; the height of the fracture zone was approximately ten times the mining thickness.

(2) The overlying strata can be divided into arched caving zone, wavy bending zone, and synchronous bending zone according to the structural characteristics of the overlying strata in the backfill–strip mining. Meanwhile, the movement characteristics of the three zones varied from one area to another.

(3) The main structure stratum and synchronous structure stratum played a key role in controlling partial strata deformation, which existed among the three subsidence zones. They formed the two-layer control structure in the strata. First, the main structure stratum prevented the strata from caving above itself and significantly decreased the subsidence space spread upward. Then, the synchronous structure stratum hindered the upward spread of the wavy subsidence and smoothened the overlying strata.

(4) The overlying strata of the backfill–strip mining experienced initial subsidence phase, active subsidence phase, and delayed subsidence phase during the excavation processes of the different working faces. The dynamic subsidence curves of the overlying strata were composed of several "ladder-shaped" subsidence curves, which correspond to each working face. However, the duration and subsidence extent of the "ladder-shaped" curves were different because of the different spatial relationships between the rock and mining working faces.

References

Chen SJ, Yin DW, Cao FW, Liu Y, Ren KQ (2016) An overview of integrated surface subsidence-reducing technology in mining areas of China. Nat Hazards 81:1129–1145

Cui MX, Wang JS, Chen YH (2016) Annual report on China's energy development. Social Sciences Academic Press, Beijing

Dehghan S, Shahriar K, Maarefvand P, Goshtasbi K (2013) 3-D modeling of rock burst in pillar no. 19 of Fetr6 chromite mine. Int J Min Sci Technol 23:231–236

Fang XQ, Zou YM, Cheng YW, Yang HX (2013) Research of secondary strip mining in a deep coal seam under the building structures. J Min Saf Eng 30:223–230

Gao F, Zhou KP, Dong WJ, Su JH (2008) Similar material simulation of time series system for induced caving of roof in continuous mining under backfill. J Cent South Univ T 15:356–360

Ghabraie B, Ren G, Zhang X, Smith J (2015) Physical modelling of subsidence from sequential extraction of partially overlapping longwall panels and study of substrata movement characteristics. Int J Coal Geol 140:71–83

Ghasemi E, Ataei M, Shahriar K (2014) An intelligent approach to predict pillar sizing in designing room and pillar coal mines. Int J Rock Mech Min 65:86–95

Gu DZ (1995) Similar material and similar model. China University of Mining and Technology Press, Xuzhou

Guo GL, Wang YH, Ma ZG (2004) A new method for ground subsidence control in coal mining. J China Univ Min Technol 33:150–153

Guo WJ, Zhang XG, Shi JW, Li YY (2010) Present situation of research on backfilling mining technology in mines and its application prospect. J Shandong Univ Sci Technol 29:24–29

He GQ, Yang L (1991) Mining subsidence. China University of Mining and Technology Press, Xuzhou

Industry SBOC (2000) The regulation of leaving coal pillar and mining coal of holding under the buildings, water bodies, railways and the main roadway. Coal Industry Press, Beijing

Li HC (1988) Similar material simulation experiment of rock pressure. China University of Mining and Technology Press, Xuzhou.

Liu PL (2014) Research on characteristics of surface movement and deformation in full-pillar mining with wide strip filling. China Coal 40: 9–12

Lokhande RD, Prakash A, Singh KB, Singh KK (2005) Subsidence control measures in coalmines: a review. J Sci Ind Res India 64:323–332

Marschalko M, Yilmaz I, Kubecka K, Bouchal T, Bednarik M, Drusa M, Bendova M (2015) Utilization of ground subsidence caused by underground mining to produce a map of possible land-use areas for urban planning purposes. Arab J Geosci 8:579–588

Mitchell RJ, Olsen RS, Smith JD (1982) Model studies on cemented tailings used in mine backfill. Can Geotech J 19:14–28

Peng SS (2013) Coal mine ground control. China University of Mining Technology Press, Xuzhou

Qian MG, Xu JL (2006) Discussion of several issues concerning the development of coal industry in China. J Min Saf Eng 32:127–132

Sun XK, Li XH (2008) The new technology of waste-filling replacement mining on strip coal pillar. J China Coal Soc 33:259–263

Wu K, Cheng G, Zhou D (2015) Experimental research on dynamic movement in strata overlying coal mines using similar material modeling. Arab J Geosci 8:6521–6534

Xu JL, Lai WQ, Zhu WB (2004) Status of coal mining industry in China. J Mines Met Fuels 52:395–398

Xuan D, Xu J, Zhu W (2013) Backfill mining practice in China coal mines. J Mines Met Fuels 61:225–234

Zha JF (2011) Mining subsidence control theory and application of solid backfilling. China University of Mining and Technology Press, Xuzhou

Zha JF, Guo GL, Feng WK, Wang Q (2011) Mining subsidence control by solid backfilling under buildings. Trans Nonferrous Met Soc 21:670–674

Zhang DH, Liang J, Guo C, Liu JW, Zhang XQ, Chen ZX (2010) Exploitation of photogrammetry measurement system. Opt Eng 49:37005

Zhu X, Guo G, Zha J, Guo Q (2015) Optical image method to deformation monitoring of similar material model. J China Univ Min Technol 44:176–182